Nd:YAG Light Source and External Modulator for A VSB-AM Video Transmitter: A Performance Evaluation

Y. Trisno and D. Grubb III
General Instrument Corporation
Jerrold Communication Division

ABSTRACT

A miniature Nd:YAG laser and an intensity modulator based VSB-AM video signal transmitter is described. With a light source having RIN level below -170 dB/Hz, the system allows a relatively low modulation index to be used. For a 40 channel system using a standard MZ, a CTB= 60 dB corresponds to m_i= 1%. With 75 mW Nd:YAG laser source, a system with power budget of 5.5 dB and 50 dB CNR is realizable. Several promising techniques of modulator linearization are also given.

INTRODUCTION

The development of optical transmitter for VSB-AM video transmission has been mostly based on direct modulation of DFB lasers. An alternative design approach is to use an external modulator and the relatively high power Nd:YAG laser as the CW optical source. In this way, the stringent linearity requirement on the laser can be removed.

This paper presents the analysis of an optical VSB-AM video transmitter based on the Nd:YAG laser and the intensity modulator. It is divided into four separate sections which are outlined next. We begin by describing the characteristics of a Nd:YAG laser as an optical source for this application. The analysis of the intensity modulator will then follow. After describing the components of the transmitter, the system level performance is analyzed. Finally, different techniques of modulator linearization to improve the CTB performance are described.

LIGHT SOURCE

While the source linearity is no longer an issue in this transmitter design, many of the laser parameters such as noise, optical spectrum, and linewidth together with the available power are still critical. For the Nd:YAG laser measurement of the aforementioned parameters was performed. First, the noise component originating from the laser unit is addressed. Then the effect of the optical spectrum on the amount of power coupled into the fiber will be discussed.

The RIN is measured under three different measurement conditions. First a back to back (with attenuator and minimum amount of back reflection) measurement is done from 50 MHz to 1GHz. Under this condition, the laser RIN is measured better than -173 dB/Hz which is our measurement system limit.

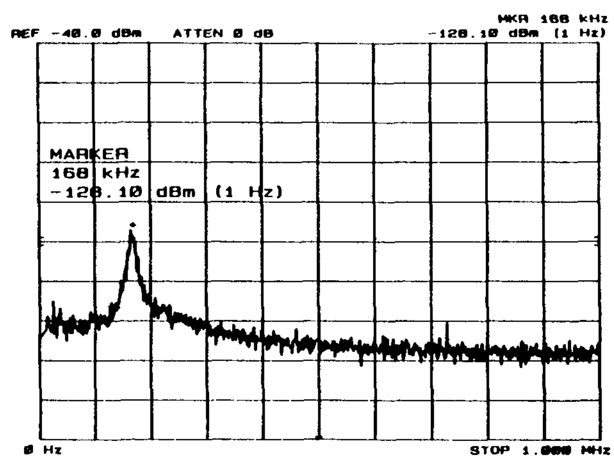

Figure 1. The relaxation oscillation of the Nd:YAG laser unit used in this experiment

Next a 35 kM link of standard SM fiber is used. In this case no degradation in RIN is measurable with negligible external back reflection (BR). However, with the presence of BR laser RIN degrades non uniformly. The worst measured value is -162 dB/Hz. Based on this result an optical isolator is necessary for this application. There is also no mode partition noise observed in the last measurement.

The second noise source arises from the relaxation oscillation frequency (ROF) of Nd:YAG laser system which occurs at around 170 kHz for the unit on hand, Figure 1. After RF modulation, this ROF frequency is shifted up to the RF domain and is located at ± 170 kHz around the modulating RF carrier. Figure 2 shows the shifted ROF around a modulating carrier at frequency of 250 MHz. The relative level of the carrier to the noise is ≈65 dBc. It is clear from the figure that the translated ROF will be an additional noise rather than an addition to CTB (the spectrum beneath the carrier) level.

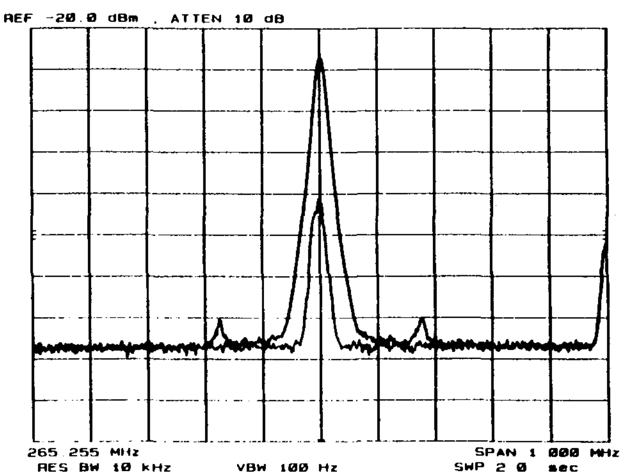

Figure 2. The up converted laser ROF after being modulated by a tone at 250MHz

Further measurements were performed for different modulation index and different frequencies (450 MHz, m= 0.3). The result is shown in Figure 3. The relative level of the carrier and the noise stays relatively constant [1]. At this level, this noise is not expected to affect the picture quality in an VSB-AM video transmission application. If it is absolutely required to remove this type of noise, an optoelectronic feedback loop could be used to cancel it [2].

In the diode pumped laser, relatively high level of current is involved to drive the pump laser diode, therefore it is necessary to reduce the excess electronic noise from the power supply unit. Otherwise, the noise could propagate into the Nd:YAG laser output if it falls into the proper frequency range. Figure 4 shows the measurement result of this type of excess noise. As shown in the figure, it will contribute significantly to the CTB. However, this type of noise is not a fundamental phenomena and is easily corrected.

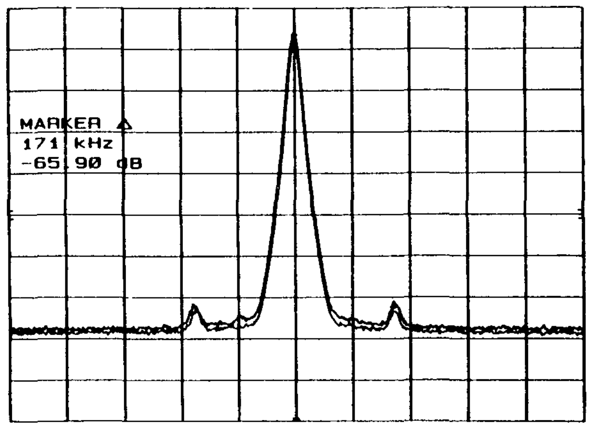

Figure 3. A similar measurement as in in the Fig. 2 for m= 0.3 and F= 450MHz

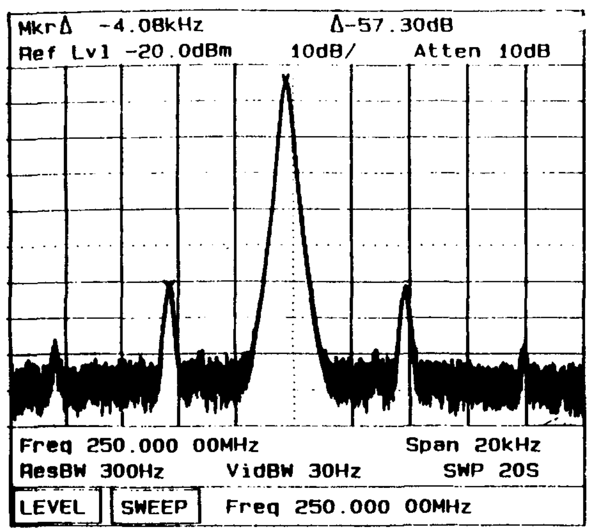

Figure 4. A low frequency excess noise originated from the pump laser diode circuitry

One of the potential advantages of using Nd:YAG laser is to extend the available power budget for the AM link. Currently the available power ranges from 50 to 200 mW. For long distance (greater than 20KM) application the optical spectrum of the laser becomes important to avoid nonlinear SBS threshold of the fiber [3]. Among the Nd:YAG products available, that with a single line at 1319 nM with several longitudinal modes (total spectrum of ≈4Å) is the optimum candidate.

In summary, a Nd:YAG laser is an attractive choice of light source for high power VSB-AM video transmission system. It has many of the desirable characteristics sought for this application. Unfortunately, an external modulator is required to impress the video information. Therefore a linear optical intensity modulator must be developed. This is the focus of the next section.

INTENSITY MODULATOR

There are many different categories of optical intensity modulators [4] to [6]. At present the Lithium Niobate based modulators are readily obtainable as advanced R&D product from few different suppliers. Consequently this section mainly focusses on the Lithium Niobate based modulator. In particular, the performance of a Mach Zehnder (MZ) type modulator will be analyzed.

A MZ intensity modulator is basically an implementation of a Mach Zehnder interferometer in a planar wave guide form. The optical output power as a function of the modulating carrier voltages can be expressed as in equation (1).

$$P_o = P_b\left[1 + Cos\left\{\phi_i + \phi_b + \frac{\pi}{V_\pi} \cdot \sum_{i=1}^{N} m_i V_i \, Sin(\omega_i t + \theta_i)\right\}\right] \quad (1)$$

Instead of directly attempting to analyze the distortion components from equation (1), it is simpler and more elegant to work using single carrier modulation. Based on the known relation between the composite distortion and the harmonic, the expression for CTB will then be derived. For linear analog applications, a MZ modulator is biased at the quadrature point of its response curve. If this point is stable, the first two arguments in the cosine function will be equal to integer multiple of $\pm\pi/2$ depending on the bias point selected. Performing trigonometric expansion on equation (1) and then writing the result in term of the first three components of its series approximation yields the next two equations.

The fundamental component is:

$$\left[KV_m + \frac{(KV_m)^3}{8}\right] \cdot Sin\ \omega t \quad (2)$$

The third harmonic component is:

$$\frac{(KV_m)^3}{24} \cdot Sin 3\omega t \quad (3)$$

where

$$K = \frac{\pi}{V_\pi}$$

$$V_m = m \cdot V_p$$

The parameters K and V_m are the device and modulation index dependent variables respectively. To convert equation (3) into a CTB expression two additional variables must be known. The first is the relation of the third harmonic to the CTB. It can be shown that each CTB is 15.56 dB higher than the third harmonic. The other is the number of triple beats that fall onto the particular frequency being monitored. The result is equation (4) [7].

$$CTB|_{Freq} = 20 \cdot \left(\frac{Fundamental}{3^{rd}\ Harmonic}\right) + 10 \cdot Log(N) + 15.56 \quad (dBc) \quad (4)$$

where N is the number of triple beats that fall onto the desired frequency.

In practice, the quadrature point may not be stationary due to several drifting mechanisms in the device. This drift causes an increase in the second order distortion. The permissible level of drift depends on the CSO being specified. Further, a large drift will also contribute to some change in the fundamental amplitude. These relations can be seen clearly from the following set of equations, which are derived from the full series expansion of equation (1).

As before the expansion is also based on a tone modulation and carried out up to third order components.

The fundamental component is:

$$\frac{K_m V \cdot Sin\,\overline{\phi}\left[-1 + \frac{3}{8}\cdot(K_m V)^2 - \frac{5}{96}\cdot(K_m V)^4\right]}{1 + Cos\,\overline{\phi}\cdot\left[1 - \frac{1}{2}\cdot(K_m V)^2 + \frac{3}{32}\cdot(K_m V)^4\right]} \quad (5)$$

The second harmonic component is:

$$\frac{\frac{1}{4}\,(K_m V)^2\cdot Cos\,\overline{\phi}\left[1 - \frac{1}{3}\cdot(K_m V)^2\right]}{1 + Cos\,\overline{\phi}\cdot\left[1 - \frac{1}{2}\cdot(K_m V)^2 + \frac{3}{32}\cdot(K_m V)^4\right]} \quad (6)$$

The third harmonic component is:

$$\frac{\frac{1}{24}\,(K_m V)^3\cdot Sin\,\overline{\phi}\left[-1 + \frac{5}{16}\cdot(K_m V)^2\right]}{1 + Cos\,\overline{\phi}\cdot\left[1 - \frac{1}{2}\cdot(K_m V)^2 + \frac{3}{32}\cdot(K_m V)^4\right]} \quad (7)$$

where

$$\overline{\phi} = \phi_i + \phi_b$$

When the angle ϕ is equal to $\pi/2$, the above set of equations reduce to the previous equation set (2) to (3). To compute CTB equation (4) is still valid provided it is replaced by equation (5) and (7) respectively.

Before proceeding to present the theoretical plot of MZ distortion as a function of modulation index, we would like to discuss the experimental characterization of a MZ. The parameters of interest at this state of evaluation are the third order distortion performance and the second order distortion vs bias point. For a CTB measurement, the MZ is biased in the neighborhood of its quadrature point. The modulation index of the modulating RF signal is set by a computer controlled RF attenuator. Figure 5 shows a typical plot of the CTB versus modulation index. The abscissa represents the individual modulation index assuming the carrier has a Gaussian distribution [3]. A comparison between the experimental result and the theoretical calculation is displayed in Figure 6 for 40 channel carriers. From

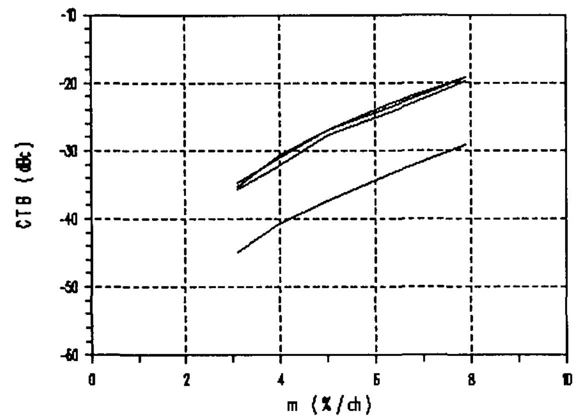

Figure 5. A typical CTB level of a MZ under 40 channel modulation

the figure it is apparent that good agreement is achieved between them. This eliminates the need of multi carrier generator requirement to perform this measurement. Therefore much simpler experimental set up can be used.

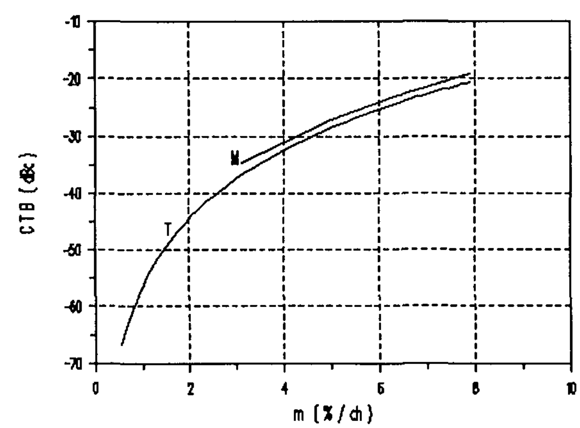

Figure 6. Comparing the theoretical calculation (T) and measurement (M) values of CTB vs m.

Measurement of CSO is done rather differently. For this measurement the RF attenuator is set at a fixed value. The MZ bias level is swept between a given voltage range. The result is shown in Figure 7. The upper graph is the carrier and the lower one is the composite second order components at a given frequency. Each pair of graphs (carrier and distortion) represents a specific frequency band being tested. The bias voltage is stepped in 10 mV increments. The best CSO is approximately 65 dBc which can be seen directly from the plot. For this case, the bias drift tolerance is in the order of 20 mV.

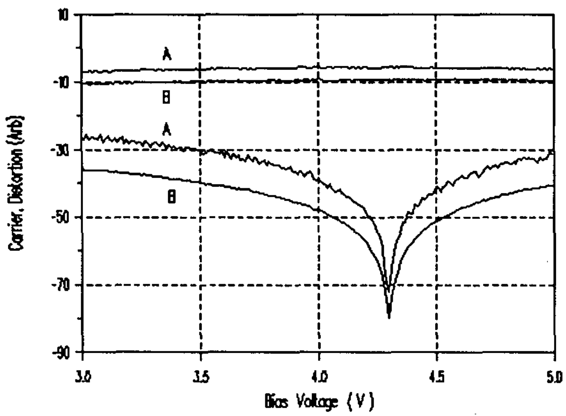

Figure 7. The second order distortion versus bias voltage of a MZ

SYSTEM LEVEL PERFORMANCE

In this section the various parameters of both the light source and the modulator which are related to the system performance are detailed. Specifically, the influence of the RIN, the modulation index, the CTB, and the system power budget on the system performance will be considered. Finally, an example of system design calculation based on two graphs is presented.

Assuming the MZ is perfectly linear, then for modulation index exceeding a certain threshold, the only distortion components are due to the non linear clipping induced distortion (CID) at both lower and upper portion of a MZ transfer function. For single clipping region and further assuming large number of channels (greater than 10) Saleh [8] and Grubb and Trisno [3] show the threshold of the RMS modulation index is 0.246. This number corresponds to a 5.5 % modulation index for each channel in a 40 carriers transmission system. For the MZ case, the RMS modulation index will be 3 dB lower.

The central issue of the analysis is to find the relation between the CNR and the CTB for a power budget, laser output power, and laser RIN. Figure 8 is a plot of the CNR versus power budget. It is calculated based on the parameters given below. The laser output power is 75 mW. The laser RIN is 170 dB/Hz. The modulator parameters are given as follows. The fiber to fiber insertion loss is 6 dB. The experiment uses 40 channel modulating carriers. A standard MZ modulator device is used. The receiver thermal noise is 7 pA/√Hz. Each pair of graphs corresponds to a specific modulation index. The upper curve of each pair represents the shot noise limit for that particular modulation index. Graph A, B, and C correspond to modulation index of 4, 3, and 1 % per channel respectively.

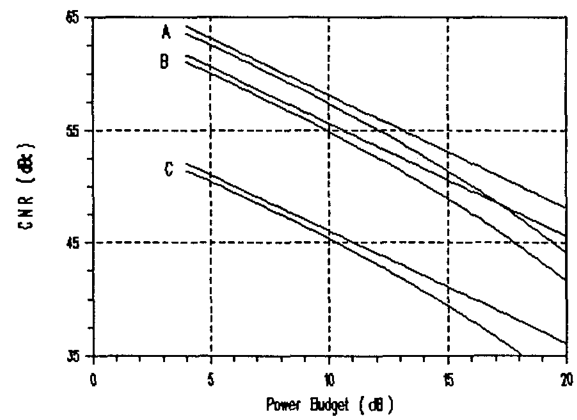

Figure 8. The CNR plot as a function of system power budget for different m.

Using the above graphs and the distortion (CTB) versus modulation index plot (Figure 6), the desired system performance can be easily estimated. For example, a system using a standard MZ and Nd:YAG source having parameters mentioned above, m= 1% (Figure 6) is required to reach a CTB level of 60 dB. Using Figure 8, a CNR= 50 dB corresponds to a 5.5 dB system power budget. For a linearized modulator, the pair of graphs can still be used provided the CTB versus m plot is updated for the corresponding condition.

MODULATOR LINEARIZATION

Comparing the measured (also the theoretical) third order distortion to the generic VSB-AM system specification, some forms of modulator linearization will be required if more efficient device utilization is desired. Fortunately, many compensation techniques can be used because of the repeatability of the MZ response. Basically, there two different approaches. First is the use of electronic techniques such as feed forward and predistortion methods. The other is optical compensation approach. In this section each of these methods based on published experimental data are reviewed.

Johnson and Roussell of Lincoln lab [9] showed that by adjusting the amount of TE and TM mode content in the MZ and setting the proper biasing for each of the modes for optimum cancellation, a respectable 20 dB of compensation can be obtained. While their result was derived from rather low frequency measurements, it is believed that similar result can be readily obtained with measurement in the CATV frequency band. One potential cause of system performance degradation is during the transmission over long fiber. The fact that the TM mode is a slightly higher order mode than the TE mode implies that the TM mode will be more susceptible to bending loss. The actual effect due to this potential problem must be measured experimentally.

Another simple linearization techniques is to use an electronic predistortion circuit. Childs and O'Byrne [1] have used a pair of diode strings to generate the required level of predistorted signal to compensate the MZ response curve. Their measurement is done under modulated video conditions. For 3.3% of modulation index per channel (of 50 channels), a 60 dBc CTB level is achieved. This corresponds to a 16 dB improvement from the standard MZ curve.

Still another approach is to employ a hybrid ooptoelectronic feed forward network. Ridder and Korotky [10] have experimented with one version of this approach. Basically, it uses a pair of identical MZ to first generate the distortion component which will then be used to compensate the second MZ. The CTB improvement in this case is in the order of 15 dB across the 50 to 300 MHz range, the same order of magnitude of improvement as in the previous case.

In summary, many different approaches of third order distortion compensation can be done for the MZ modulator. By combining some of this techniques, a better compensation level could be obtained. To reach the optimum modulation index operation, another 10 to 15 dB improvement is required.

SUMMARY

In this paper components making up a VSB-AM transmitter based on the Nd:YAG laser and the intensity modulator have been described. Additionally, various trade offs among parameters which influence the system level performance were discussed. Finally, a comparison among different techniques of modulator linearization have been presented. The key to the success of this type of transmitter is the availability of linear or linearized intensity modulators.

ACKNOWLEDGEMENT

The authors wish to thank Hank Achor for valuable discussion and his time for proof reading this paper.

REFERENCES

1. R.B. Childs and V.A. O'Byrne, "50 Channel VSB-AM Transmission Employing a Linearized External Modulator," Proc. OFC 1990, Jan 22 - 26 1990, San Francisco, CA, paper PDP-23.

2. T.J. Kane, "Diode Pumped Laser as Sources for Fiber and Space Communications," Proc. 1989 LEOS Ann. Meeting, Oct 17 - 20, 1989, Orlando, Fl, paper ELT3.4.

3. D. Grubb III and Y. Trisno, "AM Fiber Optic Trunks - A Noise and Distortion Analysis," Proc. NCTA 1989, May 21 - 24 1989, Dallas, TX.

4. R.V. Johnson, "Recent Developments in Integrated Optics at Crystal Technology," Proc. Integrated Optics and Optoelectronis, Sept 5 - 8 1989, Boston, MA, SPIE Vol. 1177, pp 327-33.

5. L. D. Hutcheson, ed., Integrated Optical Circuit and Components, 1987, ch. 7, pp 169-228.

6. T. Tamir, ed., Integrated Optics, 2nd ed., Springer Verlag, NY 1985

7. Y. Trisno, "A Brief Summary on Ti:LiNbO$_3$ Mach Zehnder Modulator Devices Characterization," Unpublished internal report.

8. A.A. Saleh, "Fundamental Limit on Number of Channels in Subscarrier Multiplexed Lightwave CATV System," Elect. Lett., vol 25, no. 12, pp 776-777, June 1989.

9. L.M. Johnson and H.V. Roussell, "Reduction of Intermodulation Distortion in Interferometric Optical Modulators," Optics Lett, vol. 13, no. 10, pp 928-30, Oct 1988.

10. R.M. Ridder and S. Korotky, "Feedforward Compensation of Integrated Modulator Distortion," in Proc. OFC 1990, San Franscisco, CA, Jan 22-26 1990, paper WH5.